

Exact Zero-Field Hopping Rates in a Gaussian Energy Distribution

Z.G. Soos and J.M. Sin
Department of Chemistry, Princeton University
Princeton, NJ/USA

Abstract

Models of photoconductors used in xerography are based on donors with a Gaussian energy distribution whose width is inferred from the zero-field mobility, μ(T). Exact mean dwell times for Marcus, Miller-Abrahams and symmetric rates are obtained at zero field for lattices with energetic, positional and orientational disorder. Monte Carlo simulations of μ(T) and hopping rates bring out the role of disorder-induced steps. Evidence for such steps in molecularly doped polymer comes from the concentration dependence of μ(T). Transport involves fast, repetitive steps with small displacement and geometrical disorder increases the T dependence of μ(T). Present analyses of μ(T) overestimate energetic disorder.

1. Introduction

Time-of-flight (TOF) experiments measure the mobility μ(E,T) of holes in molecularly doped polymers (MDPs), the photoconductors used in xerography.[1-5] The transit time $t_{1/2}$ for crossing a film of thickness L in applied field E gives $\mu = L/Et_{1/2}$. Similar mobilities with remarkable E and T dependencies are found for many donors and polymers. The Gaussian disorder model of Bässler and coworkers[2,3] focuses on hopping between sites with a normal energy distribution g(ε,σ) and $\sigma \sim 10^3$K. The physical picture of localized states, nonadiabatic hole transfer and g(ε,σ) is widely used and retained in this paper. It is consistent with, but leaves open, such basic issues as the rate law for hopping, the nature of geometrical disorder, the origins of energetic disorder and specific donor-polymer interactions. The zero-field μ(T) inferred from E > 0 data has a special role experimentally: the slope of lnμ(T) vs. T^{-2} is $^2 -4\sigma^2/9k^2$ or, alternatively, the slope vs. T^{-1} is[5] the activation energy in polaron models.

We present below a new theoretical approach to μ(T) that proves geometrical as well as energetic contributions to the slope of lnμ(T). Our analysis brings out the role of disorder-induced steps and accounts naturally for published data on variable donor concentration in the same polymer.

Monte Carlo (MC) simulations of random walks (RWs) have been used to model the mobility.[1-3] The limitations of MC are slow convergence and having to specify all parameters at the outset. Comparison with experiment has necessarily been indirect. We also require RWs for μ(T). In addition, we obtain the exact zero-field dwell time, ⟨τ(β)⟩, for g(ε,σ) and Miller-Abrahams (MA), symmetric and Marcus or small polaron rates. Analytical results lead to disorder-induced steps and to revised interpretation of MDP transport.

Our treatment rests on normal transport and thermal equilibrium. The appearance of $t_{1/2}$ in linear plots of current vs. time indicates normal transport in MDPs, with finite dwell time ⟨τ(E,T)⟩ and displacement ⟨z(E,T)⟩ per step after many steps. Normal transport is assured[6] for a Gaussian g(ε,σ), but the time scale is set by disorder and diverges as $\beta\sigma \to \infty$. The mobility and its E = 0 limit μ(T) are

$$\mu(E,T) = \frac{\langle z(E,T)\rangle}{E\langle \tau(E,T)\rangle} \to \left(\frac{\partial \langle z(E,T)\rangle}{\partial E} \right)_0 / \langle \tau(T)\rangle \qquad (1)$$

Early work on inorganic photoconductors showed dispersive transport, for which (1) fails and transit times require log-log plots. Scher and Montroll[7] introduced a continuous time RW with *divergent* ⟨τ(T)⟩ for dispersive transport, which Schmidlin[8] related to an *exponential* energy distribution. Normal transport is expected for Gaussian g(ε,σ) and confirmed in MDPs by TOF profiles that become broad or dispersive only in thin films, at low T or at high field.

The Einstein relation between mobility and diffusion shows that z_0(E,T) for the *ordered* lattice goes as E/T. The ratio χ(E,T) = z_0(E,T)/⟨z(E,T)⟩ > 1 represents reduced motion due to disorder or, alternatively, to extra steps for the same displacement. The zero-field mobility is formally

$$\mu(T)T / T_r = \langle \tau(T)\rangle^{-1} \chi(T)^{-1} = p_e(T) / \tau_0 \chi(T) \qquad (2)$$

with $T_r = ea_0^{\ 2}/6k$ for charge e and mean-square displacement $a_0^{\ 2}$. The ordered lattice has χ = 1, shorter $\tau_0 = \langle \tau(T)\rangle / p_e(T)$ with $p_e(T) < 1$, and spacing $a < a_0$ when steps beyond first neighbors are allowed. Young[9] took T_r = 295K and assigned σ from the slope of $\ln T\mu/T_r$ vs. T^{-2}. The mobility (2) requires no assumption beyond normal transport.

As shown in Section 2, the zero-field hopping rate, $\langle \tau(T)\rangle^{-1}$, follows from thermal equilibrium and detailed balance. Now g(ε,σ) facilitates analytical results for standard rates in an infinite lattice with energetic, positional and orientational disorder. RWs with the same parameters in

finite lattices converge[10] to $\langle\tau(T)\rangle$ and yield $\chi(T)$. We interpret disorder-induced steps in Section 3 with the aid of an auxiliary lattice whose spacing a' > a_0 increases with the overall disorder. In Section 4 we turn to mobility data in MDPs with variable donor concentration and show that disorder-induced steps reduce $\mu(T)$ more than dwell times.

2. Mean Dwell Time in Zero Field

We model MDPs by lattices with spacing a ~ 8Å that approximate the density. Donors (D) randomly fill a fraction p of sites; the polymer (P) fills the rest and has no role in the transport. The hopping rate ω_{nm} between donors at n and m depends on distance, orientation and energy. Physical considerations suggest an exponential in r_{nm} and $\tau_r = 1/\Sigma_m\omega_{rm}$ has rates to nearby D's with energies chosen from $g(\varepsilon,\sigma)$. The random variables for position, energy and orientation are independent by hypothesis. We consider an infinite RW generated by ω_{rm}. Normal transport at E = 0 indicates an equilibrium system. The transport does not depend the starting point and the time spent at sites is Boltzmann distributed for rates that satisfy detailed balance.

Different τ_r at isoenergetic sites clearly implies a probability that goes as $1/\tau_r$; sites with short dwell times are reached more often. Normalization gives $\tau(\varepsilon)$

$$\tau(\varepsilon)^{-1} = \left\langle \tau_r^{-1} \right\rangle_\varepsilon = \left\langle \sum\nolimits_m \omega_{rm} \right\rangle_\varepsilon \qquad (3)$$

The average over sites with $\varepsilon_r = \varepsilon$ can be taken step by step. The geometrical factors are $p\langle\Omega\rangle\exp(-\gamma r_m)$, where $\langle\Omega\rangle$ is an orientational average, while the energy average is over $g(x,\sigma)$ for rate $\omega(\varepsilon,x)$ to a site with $\varepsilon' = x$. We have

$$\tau(\varepsilon)^{-1} = p\langle\Omega\rangle\left(\sum\nolimits_m \exp(-\gamma r_m)\right)\int_{-\infty}^{\infty} dx g(x,\sigma)\omega(\varepsilon,x) \qquad (4)$$

The $\omega(\varepsilon,x)$ factors for Marcus rates with reorganization energy λ, symmetric and MA rates are, respectively,

$$\ln\omega(\varepsilon,x) = -\beta(\lambda-\varepsilon+x)^2/4\lambda, \quad \beta(\varepsilon-x)/2, \ \textit{and} \quad \beta(\varepsilon-x) \ \textit{for}\ x>\varepsilon, \quad 0 \ \textit{for}\ x\le\varepsilon \qquad (5)$$

The integrals over $g(x,\sigma)$ are elementary.

The RW generates a unique distribution $h(\varepsilon)$ of visited sites for normal transport. Although $h(\varepsilon)$ and $\tau(\varepsilon)$ depend on the rate law, detailed balance implies that $h(\varepsilon)\tau(\varepsilon)$ goes as $g(\varepsilon,\sigma)\exp(-\beta\varepsilon)$. The mean dwell time is

$$\langle\tau(\beta)\rangle = \int_{-\infty}^{\infty} de h(\varepsilon)\tau(\varepsilon) = h(0)\tau(0)\sqrt{2\pi\sigma^2}\,\exp(\beta^2\sigma^2/2) \qquad (6)$$

The proportionality constant has dimensions of time and follows from ratios at $\varepsilon = \varepsilon$ and 0. We then obtain $h(\varepsilon)$ from $\tau(\varepsilon)$ in (4) and the product $h(\varepsilon)\tau(\varepsilon)$. The normalized distribution of visited sites for Marcus rates is[10]

$$h(\varepsilon) = (2\pi B^2)^{-1/2}\exp[-(\varepsilon+\beta\sigma^2/2)^2/2B^2]$$
$$B^2 = \sigma^2(2\lambda+\beta\sigma^2)/2(\lambda+\beta\sigma^2) \qquad (7)$$

The visited sites reduce to $g(\varepsilon,\sigma)$ at $\beta\sigma = 0$, when energetic disorder is irrelevant. The peak shifts to $-\beta\sigma^2/2$ and $h(\varepsilon)$ narrows to $\sigma/\sqrt{2}$ at low T, where $\langle\tau\rangle$ diverges as indicated in (6). Symmetric rates lead to (7) with $B = \sigma$. For MA rates, we know[10] h(0) analytically and that suffices for (6).

The mean dwell time (6) for Marcus rates and $g(\varepsilon,\sigma)$ follows from (7) and (4),

$$\langle\tau(\beta\sigma,p,\Omega\rangle^{-1} = \tau_0^{-1}p_e(\beta\sigma,\Omega)$$
$$p_e(\beta\sigma,\Omega) = p\langle\Omega\rangle(1+\beta\sigma^2/2\lambda)^{-1/2}\exp(-\beta^2\sigma^2/4) \qquad (8)$$

The slower $\langle\tau\rangle = \tau_0/p_e$ of (2) is explicitly given by $p_e(\beta\sigma,\Omega)$, *without* having to specify the average $\langle\Omega\rangle$ or the range of steps in τ_0. We can also view p_e as dilution, since the hopping rate at constant T is proportional to the donor fraction. Other rates and $g(\varepsilon,\sigma)$ yield[10] different $p_e(\beta\sigma,\Omega)$. Symmetric rates give (8) without the square root factor. MA rates for $\beta\sigma > 2$ have $1/\beta\sigma$ instead of the square root; the full expression is complicated but readily evaluated. The rates leave open the choice of $\langle\Omega\rangle$ or τ_0.

The $-\ln\langle\tau\rangle$ vs. $\beta^2\sigma^2$ plots in Fig. 1 show (8) for the three rates and have a common origin, $\ln p\langle\Omega\rangle$. The range to $\beta\sigma = 4$ covers most MDP data and $\lambda \sim 2\text{-}3\sigma$ is typical. The slope vs. $\beta^2\sigma^2$ is exactly –1/4 for symmetric rates, as given by p_e, but only approximately –1/4 for Marcus or MA rates. We note, first, that the expected slope of –1/2 suggested by (6) is reduced for all three by the T dependence of $h(\varepsilon=0)$ and $\tau(\varepsilon=0)$ and, second, that T^{-2} extrapolations are not exact for MA rates. A Gaussian $g(\varepsilon,\sigma)$ is convenient for exact zero-field hopping rates that are products of energetic and geometrical factors.

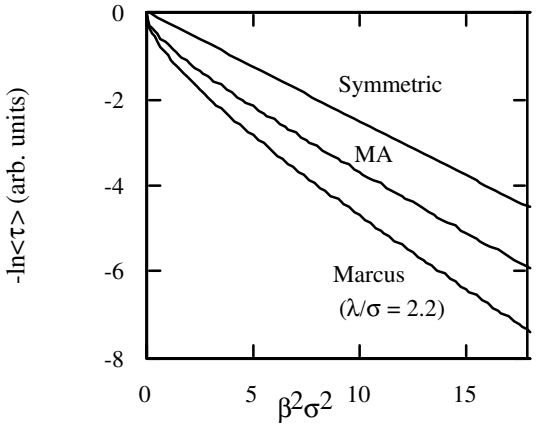

Figure 1. Exact hopping rates, Eq. (8), for g(ε,σ) and symmetric, MA or Marcus rates; the origin is ln p < Ω>z.

3. Disorder-Induced Steps

The mean dwell time increases by $1/p_e(\beta\sigma,\Omega)$ at E = 0 and normal transport implies eventual convergence to $\langle r^2\rangle$ per step. Disorder generates a distribution $\{\omega_m\}$ of rates at each site and strongly correlates successive steps. The quantitative measure of extra steps is[10]

$$\chi(\beta\sigma, p, \Omega)^{-1} = \left\langle r^2 \right\rangle / a_0^2 \qquad (9)$$

where $a_0^2 \geq a^2$, the mean square displacement per step of the ordered system, is slightly larger than a for $\exp(-\gamma a)$ with $\gamma a \sim 7$. To simulate χ, we generate RWs and record the position after groups of N_0 steps, with $N_0 = 10^4$ or 10^5 steps, respectively, for modest and strong disorder. An N-step walk gives N/N_0 displacements whose average per step is $\langle r^2\rangle$.

Normal transport ensures convergence for sufficiently large N and N_0 that, however, increase rapidly with disorder. Thermodynamic simulations[11] for $g(\varepsilon,\sigma)$ fail in finite lattices with increasing $\beta\sigma$ because there are too few sites below the mean energy, $-\beta\sigma^2$. Diffusion simulations[12] fail as $p \rightarrow 0$, even without energetic disorder, because $\langle r^2\rangle$ requires very long RWs. We keep track of the mean dwell time, its second moment, and several energy moments of visited sites. Convergence with N to $\langle\tau(\beta)\rangle$ in (8) and $h(\varepsilon)$ in (7) gives strong checks.[10] We increase N_0 until the decrease of $\langle r^2\rangle$ is small, but convergence remains an issue.

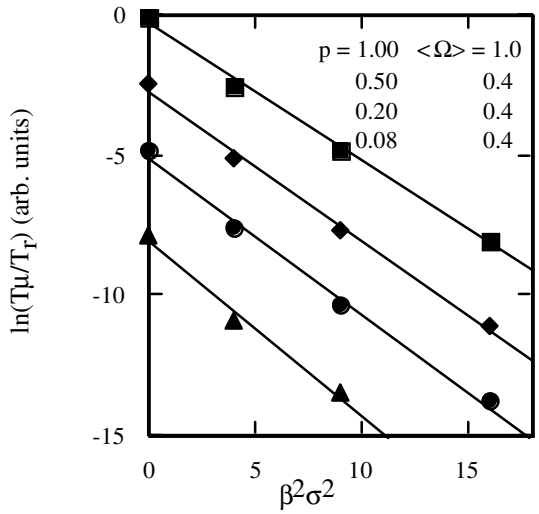

Figure 2. Zero-field mobility, Eq. (2), for $g(\varepsilon,\sigma)$ and the Marcus rates with geometrical disorder p, $\langle\Omega\rangle$. The points are Eq. (8) and simulated χ in Eq. (9); the lines are least squares fits..

Quite generally, $\chi(\beta\sigma,p,\Omega)$ increases with disorder. The $\ln T\,\mu(\beta\sigma,p,\Omega)/T_r$ vs. $\beta^2\sigma^2$ results in Fig. 2 are based on exact $\langle\tau\rangle$ and simulated χ for Marcus rates with $\sigma = 10^3$K, λ = 0.2 eV, γ^{-1} = 1.2Å, an fcc lattice with $a = (12/\sqrt{2})$Å, and the indicated p and $\langle\Omega\rangle$ for a simple model of orientational disorder.[13] Geometrical disorder (p, $\langle\Omega\rangle < 1$) increases the slope by ~20%. Previous assignments of σ or activation energies from such slopes are too high. At fixed σ and $\langle\Omega\rangle$, $\mu(T)$ at p = 0.50, 0.20 and 0.08 illustrates the concentration dependence discussed in Section 4.

Disorder reduces the mobility by slower hopping $p_e(\beta\sigma,\Omega)$ in (8) and extra steps $\chi(\beta\sigma,p,\Omega)$. Extra steps dominate at E = 0, as shown below. Although easily understood, the role of disorder-induced steps is difficult to quantify. To facilitate the interpretation of χ, we use it to *define* an ordered lattice with the same $\mu(T)$, spacing a' and nearest-neighbor steps. The reduction due to disorder leads to

$$p_e(\beta\sigma,\Omega) / \chi(\beta\sigma, p, \Omega) = (a'/a_0)^2 \exp[-\gamma'(a'-a_0)] \qquad (10)$$

We solve for a'/a_0 and list results in Table 1.

Table 1. Simulated a'/a_0, Eq. (10), for Marcus rates for the systems in Fig. 2.

$\beta\sigma$	p = 1.0 $\langle\Omega\rangle$ = 1.0	p = 0.50 $\langle\Omega\rangle$ = 0.4	p = 0.20 $\langle\Omega\rangle$ = 0.4	p = 0.08 $\langle\Omega\rangle$ = 0.4
0.2	1.00	1.44	1.85	2.36
2.0	1.29	1.74	2.15	2.69
3.0	1.59	2.08	2.51	3.00
4.0	2.04	2.54	2.95	>3.4

The ordered case ($p_e = \chi = 1$) has $a' = a_0$. The rhs of (10) decreases with a' for $\gamma' a_0 > 2$, which is well satisfied[10] by $\gamma' a_0 \sim 7$ in MDPs and $\gamma' \sim 0.95\gamma$. The point is that known p_e and simulated χ uniquely fix a'. On the contrary, $a' > a_0$ merely specifies the disorder level produced by some combination of energetic and geometrical disorder. The auxiliary lattice has the same $\mu(T)$ by construction, but entirely different dynamics. We are replacing extra steps at rate $\langle\tau\rangle^{-1}$ with slow steps $\exp(-\gamma' a')$ in a lattice whose mobility is elementary.

Modest disorder $a'/a_0 < 2$ perturbs the three-dimensional RW. The mean separation increases as $c = ap^{-1/3}$ in MDPs and as $a_0 p_e^{-1/3}$ in the auxiliary lattice. The $p_e > 0.1$ entries in Table 1 are 20-30% less than the mean separation, which gives a lower bound for μ. For stronger disorder, a'/a_0 increases more slowly as $p_e^{-1/6}$. The range of disorder in Table 1 can be approximately fit[10] to

$$\frac{a'}{a_0} = \frac{(2+\beta^2\sigma^2)p_e(\beta\sigma,\Omega)^{-1/3}}{1+(1+\beta^2\sigma^2)p_e(\beta\sigma,\Omega)^{-1/6}} \qquad (11)$$

We reiterate that χ gives a' in (10). Thus (11) is actually an interpolation suggested by the auxiliary lattice.

4. Discussion

We summarize in Table 2 dilution studies of D(p):P(1-p) systems with variable donor concentration. The donors are aromatic amines whose acronyms are given in the refs.; PS is polystyrene and PC is polycarbonate. The indicated range corresponds to modest disorder for p > 10%, when a D neighbor is likely, and extends to p = 1.7%. Dilution is

typically shown as $\ln\mu_0/c^2$ vs. $c = ap^{-1/3}$, the mean separation between donors. The prefactor mobility μ_0 is the intercept at $T^{-2} = 0$. The slopes are taken as wavefunction overlap, but extra steps due to disorder is the proper interpretation.

The implicit rationale for $\ln\mu/c^2$ vs. c plots is clearly another lattice with c > a and slow steps. The simple scaling with p is generalized in $p_e(\beta\sigma,\Omega)$ to incorporate dilution due to anisotropic hopping or low-energy sites at low T. The slope of $\ln\mu/(a')^2$ vs. a' is $-\gamma' \sim -0.8\text{Å}^{-1}$ according to (10). Since modest disorder leads to a' ~ 1.5c, the expected slope vs. c is about -1.2Å^{-1} for all D(p):P(1-p) systems with modest disorder. The reported slopes in Table 2 are in this range and reflect, as a first approximation, the $\exp(-\gamma r)$ dependence of hopping rates. The crossover to $p_e^{-1/6}$ implied by the simulations may follow from detailed study over a wide range of p.

More quantitative results for disorder-induced steps require approximations. Plots of $\ln\mu_0(T)$ vs. T^{-2} yield $\sigma(p)$ in D(p):P(1-p) systems[2,9] and the intercept μ_0 may not be exact. Similar but not identical σ and Ω are expected on physical grounds. Equal σ, Ω at constant T leads, independent of the rate law, to simple mobility ratios for $p_1 > p_2$ in (2)

$$\ln\frac{\chi(p_2,T)}{\chi(p_1,T)} = \ln\frac{\mu(p_1,T)p_2}{\mu(p_2,T)p_1} \qquad (12)$$

Since μ and p are measured, we have a direct experimental estimate of χ.

Table 2. Mobility of D(p):P(1-p) Systems: slope of $\ln\mu_0/c^2$ vs. $c = ap^{-1/3}$

D:P	Δp(%)	Slope (Å^{-1})	Ref.
TTA:PS	1.7-50	–1.12	9
TTA:PC	10-50	–1.06	9
TAPC:PC	10-100	–1.22	14
DEH:PC	8-70	–1.18	5
MPMP:PS	20-80	–1.8	15
MPMP:PC	20-80	–1.9	15
HDZ-F:PS	7-65	–1.33	16
DEASP:PC/PS	10-70	–1.67	17
TPM:PS	10-53	–1.67	18
TASB:PS	10-50	–1.67	19

Young[9] studied TTA(p):PS(1-p) from p = 50 to 1.7%, where TTA is tritolylamine. As shown in Fig. 19 of ref. 9, μ_0 decreases by almost 10^8 over this range; $p_1/p_2 \sim 30$ is a small fraction of $\chi_2/\chi_1 \sim 10^6$. The 300K decrease in Fig. 13 is comparable, from $7.4\text{x}10^{-4}$ cm^2/Vs at p = 50% to 10^{-11} cm^2/Vs at 2 or 2.5%, whose E > 0 mobilities extrapolate to the same intercept. The dilute system again needs ~10^6 more steps. The mobility (2) is linear in $\langle\tau\rangle$, and hence in p_e, while χ is exponential in p_e in (11). Disorder-induced steps suppress zero-field transport. They are less effective for E > 0, since a forward bias eventually forces $\chi(E,T) \sim 1$.

Figure 2 parallels the TTA(p):PS(1-p) data in Fig. 13 and Table 1 of ref. 9 for p = 50, 30, 20, 10% and 200 < T < 400K. Slopes at constant σ increase with dilution. The measured slopes increase even more, by 40%, and point to increasing $\sigma(p)$. The calculated change of $\mu_0(p_1)/\mu_0(p_2)$ is 36 between 50 and 8%, while the observed change is 140 between 50 and 10%. Stronger orientational disorder may be needed. We are not aware of previous attempts to model $\mu_0(p,\Omega)$, the intercept of $\ln\mu(T)$ vs. T^{-2} plots.

Disorder-induced steps are prominent in MDP models. Fluctuations are also important in general. For $g(\varepsilon,\sigma)$ and E = 0, we found the distribution $h(\varepsilon)$ of visited sites in an infinite RW. The probability of visiting site r with ε_r goes as $\tau(\varepsilon)/\tau_r$. The hopping-rate variance is a first estimate for the widths of TOF profiles. The mean square dwell time is

$$\left\langle \tau(\beta)^2 \right\rangle = \int deh(\varepsilon)\tau(\varepsilon)\left\langle \tau_r \right\rangle_\varepsilon \qquad (13)$$

The microcanonical average of $1/\Sigma\omega_{rm}$ over $\varepsilon_r = \varepsilon$ is dominated by site with the slowest rates, which is just the opposite of the dwell time (6). Disorder rapidly increases $\langle\tau(\beta)^2\rangle/\langle\tau(\beta)\rangle^2$. For Marcus rates (5), the integral (13) diverges for $\beta\sigma^2 > 2\lambda$, as follows from the common factor of $\exp[\beta(\lambda - \varepsilon)^2/4\lambda]$ for all sites. Broad TOF profiles are expected and seen at low temperature. A Gaussian $g(\varepsilon,\sigma)$ does not ensure finite moments beyond the first. Preliminary results for dilution show (13) to be exponential as $p \to 0$. The rms time $\langle\tau(\beta)^2\rangle^{1/2}$ resembles qualitatively the dwell time τ' of the auxiliary lattice. Slow steps are crucial for transport and hopping decreases exponentially. This intuitive picture does not correspond to the postulated models, however. Zero-field hopping in MDPs hopping corresponds to fast, repetitive steps with small overall displacement.

In summary, we have found exact mean dwell times in a Gaussian energy distribution for Marcus, MA and symmetric rates in lattices with independent positional, orientational and energetic disorder. The zero-field mobility of MDPs is reinterpreted in terms of disorder-induced steps and related to an auxiliary lattice. Previous assignments of energetic disorder are upper bounds that neglect geometrical contributions. Exact dwell times show the convergence of MC simulations that generate $\chi(\beta\sigma,p,\Omega)$ numerically and that can be used for E > 0. We anticipate modeling $\mu(E,T)$ in donor:polymer systems with variable filling p.

Acknowledgments

ZGS thanks R.H. Young and G.W. Hayden for stimulating discussions and help with MDP literature and simulations during the initial phases of this work. We gratefully acknowledge support from the National Science Foundation through DMR-9530116 and the MRSEC program under DMR-9400362.

References

1. P.M. Borsenberger and D.S. Weiss, *Organic Photoreceptors for Imaging Systems*, Marcel Dekker, New York, 1993, and references therein.

2. H. Bässler, *Phys. Stat. Sol.* **(b) 175**, 15 (1993).
3. P.M. Borsenberger, E.H. Magin, M. van der Auweraer and F.C. de Schryver, *Phys. Stat. Sol.* **(a) 140**, 9 (1993).
4. L.B. Schein, *Phil. Mag*. **B65**, 795 (1992).
5. J.X. Mack, L.B. Schein and A. Peled, *Phys. Rev*. **B39**, 7500 (1989).
6. Z.G. Soos and S.J. Schmidt, *Chem. Phys. Lett*. **265**, 427 (1997).
7. H. Scher and E.W. Montroll, *Phys. Rev*. **B12**, 2455 (1975).
8. F.W. Schmidlin, *Phys. Rev*. **B16**, 2362 (1977).
9. R.H. Young, *J. Chem. Phys*. **103**, 6749 (1995).
10. Z.G. Soos and J.M. Sin, *Phys. Rev*. **B** (submitted).
11. B. Derrida, *Phys. Rev*. **B24**, 2613 (1981).
12. R. Brown and B. Esser, *Phil. Mag*. **B72**, 125 (1995).
13. Z.G. Soos, S. Bao, J.M. Sin and G.W. Hayden, *Chem. Phys. Lett*. **319**, 637 (2000).
14. P.M. Borsenberger, *J. Appl. Phys*. **72**, 5283 (1992).
15. P.M. Borsenberger, *Phys. Stat. Sol.* **(b) 173**, 671 (1992).
16. P.M. Borsenberger, E.H. Magin, J.A. Sinicropi and L.B. Lin, *Jpn. J. Appl. Phys*. (**1**) **37**, 166 (1998).
17. P.M. Borsenberger and L.B. Schein, *J. Phys. Chem*. **98**, 233 (1996).
18. E.H. Magin, W.T. Gruenbaum and P.M. Borsenberger *Jpn. J. Appl. Phys*. (**1**) **35**, 3930 (1996).
19. P.M. Borsenberger, W.T. Gruenbaum and E.H. Magin, *Physica* **B 228**, 223 (1996).

Biography

Zoltán Soos received his BA in Chemistry and Physics from Harvard in 1962 and a PhD in Chemistry from Cal Tech in 1965. He has been in the Chemistry department at Princeton University since 1966. His research interests include magnetic chains, quantum cell models, charge transfer and triplet excitons in organic salts, and correlated excited states of conjugated polymers, and low-dimensional transport. He is a member of the American Chemical and Physical Societies.

Jessica Sin received her AB in Chemistry and French from Dartmouth in 1997. She has been a graduate student in the Chemistry department at Princeton University since 1998.